Adjusted bacterial cooperation in anammox community to adapt to high ammonium in wastewater treatment plant

Yiming Feng [a,b], Lingrui Kong [a,b], Ru Zheng [a,b], Xiaogang Wu [a,b], Jianhang Zhou [a,b], Xiaochen Xu [c], Sitong Liu [a,b,*]

[a] College of Environmental Sciences and Engineering, Peking University, Beijing, 100871, China
[b] Key Laboratory of Water and Sediment Sciences, Ministry of Education of China, Beijing, 100871, China
[c] Key Laboratory of Industrial Ecology and Environmental Engineering (MOE), School of Environment Sciences and Technology, Dalian University of Technology, Linggong Road 2, Dalian, 116024, China

A B S T R A C T

Bacterial cooperation is very important for anammox bacteria which perform low-carbon and energy-efficient nitrogen removal, yet its variation to adapt to high NH_4^+-N concentration in actual wastewater treatment plants (WWTPs) remains unclear. Here, we found wide and varied cross-feedings of anammox bacteria and symbiotic bacteria in the two series connected full-scale reactors with different NH_4^+-N concentrations (297.95 ± 54.84 and 76.03 ± 34.01 mg/L) treating sludge digester liquor. The uptake of vitamin B6 as highly effective antioxidants secreted by the symbiotic bacteria was beneficial for anammox bacteria to resist the high NH_4^+-N concentration and varied dissolved oxygen (DO). When NH_4^+-N concentration in influent (1785.46 ± 228.5 mg/L) increased, anammox bacteria tended to reduce the amino acids supply to symbiotic bacteria to save metabolic costs. A total of 26.1% bacterial generalists switched to specialists to increase the stability and functional heterogeneity of the microbial community at high NH_4^+-N conditions. V/A-type ATPase for anammox bacteria to adapt to the change of NH_4^+-N was highly important to strive against cellular alkalization caused by free ammonia. This study expands the understanding of the adjusted bacterial cooperation within anammox consortia at high NH_4^+-N conditions, providing new insights into bacterial adaptation to adverse environments from a sociomicrobiology perspective.

1. Introduction

Bacteria are inherently social organisms and exist within complex networks of ecological interactions (D'Souza et al., 2018; Zhang et al., 2021a). This interaction network helps microbial communities increase their resistance to ecological disturbance (Oña and Kost, 2022) and improve community production (Preussger et al., 2020). Metabolic cross-feeding refers to the process in which bacteria exchange metabolites with other microorganisms (Freilich et al., 2011), which are essential for the growth and metabolism of bacteria, as well as expanding the niche width of cross-feeders (Oña et al., 2021; Pande et al., 2016).

Anaerobic ammonium oxidation (anammox) process represents a resource-efficient biological wastewater treatment technology (Kartal et al., 2010). The anammox process converts ammonium (NH_4^+–N) and nitrite (NO_2^-–N) into nitrogen gas (N_2), which has been confirmed to help reduce greenhouse gas emissions (Cruz et al., 2019; Ni and Zhang, 2013). Microbial cross-feedings are often observed in anammox bacteria (Lawson et al., 2017; Zhuang et al., 2022). Studies have revealed multitype cross-feedings in via of amino acids, cofactors, and vitamins within the anammox community in lab-scale reactors (Lawson et al., 2017; Ya et al., 2022; Zhao et al., 2023). Symbiotic bacteria provide folate and molybdopterin cofactor (MOCO) to anammox bacteria. These metabolites are essential for the growth and activity of anammox bacteria, as they influence carbon fixation and acetyl-coA production (Zhao et al., 2018). While cross-feedings within the anammox community have been elucidated, these studies mainly focused in lab-scale reactors. In actual WWTPs, wastewater composition and bacterial communities are more complex compared to lab-scale reactors with unstable operating conditions. Therefore, the cross-feeding patterns and symbiotic bacteria within anammox system in WWTPs would be complex.

High levels of NH_4^+-N can induce intracellular pH alterations and

proton imbalance, resulting in inhibition of cell activity (Gallert et al., 1998). It has been found the bacteria enhance the formation of biofilms to gather together for metabolite exchange to resist NH_4^+-N stress (Flemming et al., 2016; Ren et al., 2015). The upregulation of ABC transporter proteins enhances bacterial resistance to high strength NH_4^+-N, which accelerates membrane transport and promotes metabolite exchange between microorganisms (Guo et al., 2024; Okada et al., 2017). Importantly, the researchers found bacteria also respond to elevated NH_4^+-N stress by altering their co-occurrence patterns with other bacterial members (Zhang et al., 2021b). Microbial interactions including quorum sensing (QS), metabolic cross-feeding, mutualism, competition, are crucial for bacteria to resist adverse environments (Rocha-Granados et al., 2020). In anammox consortia, symbionts are auxotrophic and rely on anammox bacteria to synthesize some costly amino acids (Lawson et al., 2017). Meanwhile, symbionts provide secondary metabolites, such as folate and molybdopterin cofactor, to anammox bacteria as resource feedback (Kallistova et al., 2022; Zhao et al., 2018). These processes significantly promote the growth and activity of anammox bacteria. Under various conditions, bacteria employ different energy allocation strategies and they tend to save their own energy and preferentially allocate energy to maintain fundamental survival functions (Chen et al., 2022a; Li et al., 2022). Distinct cross-feeding patterns lead to differences in metabolic burden of bacteria (Zhao et al., 2023). Therefore, anammox bacteria may respond to adverse environments by regulating cross-feeding patterns.

Based on discrepancy in response to environmental filtration, microorganisms can be divided into specialists and generalists (Prosser et al., 2007; Xu et al., 2022). Specialists possess narrow niche widths, relying heavily on specific resources, but have strong competitive capabilities within a limited range of niches (Clavel et al., 2011; Ren et al., 2023). Generalists have relatively weak competitive abilities but can tolerate a wide range of niches (Levins, 1968). Generalists and specialists have different survival strategies and respond distinctly to environmental disturbances (Hu et al., 2023). Recent studies propose that generalists are more likely to recover from environmental disturbances, whereas specialists exhibited stronger phylogenetic signals of ecological preferences (Sriswasdi et al., 2017; Wimp et al., 2019; Yan et al., 2022). The composition of generalists and specialists has an important impact on ecosystem function, and this composition can be determined by the environment, such as pH, temperature, etc. (Gad et al., 2020). Microbial interactions can alter resource utilization within a community, so changes in the co-occurrence network may also influence the shift between generalists and specialists (Yan et al., 2022). Thus, the shift between specialists and generalists within microbial community in WWTPs may contribute to the adaptation of whole consortia to environments with high NH_4^+-N.

In this study, we investigated cross-feedings among anammox consortia in an actual anammox plants treating sludge digestion liquid. Two simultaneous partial nitrification, anammox and denitrification (SNAD) bioreactors were series connected and the influent ammonium (NH_4^+-N) concentrations of the SNAD1 and SNAD2 reactor were 1785.46 ± 228.5 and 297.95 ± 54.84 mg/L, respectively. We compared the bacterial cooperation under different NH_4^+-N conditions, revealing the important role of cooperation in anammox bacteria adaptability in the WWTP. This research enhances our understanding of cross-feedings in WWTPs and provides a new perspective for microbial adaptation strategies to high NH_4^+-N.

2. Results

2.1. Reactor performance and microbial communities

The influent NH_4^+-N concentrations of the SNAD1 and SNAD2 reactors were 1785.46 ± 228.5 and 297.95 ± 54.84 mg/L, respectively, with NH_4^+-N concentrations in the SNAD1 and SNAD2 reactor being 297.95 ± 54.84 and 76.03 ± 34.01 mg/L (Fig. 1a-b). The nitrogen removal rates (NRR) were 1432.8 ± 298.69 and 214.52 ± 88.55 mg N/L/d in these two reactors (Fig. 1c). The FA concentrations in the two reactors differed significantly ($P < 0.005$), with an FA concentration of 26.22 ± 5.45 mg/L in SNAD1 reactor and 2.25 ± 1.56 mg/L in SNAD2 reactor.

We found that the species richness of microbial communities was higher in SNAD1 reactor with higher NH_4^+-N concentration compared to SNAD2 reactor. Anammox bacteria were rarely distributed in suspended sludges (0.46% ~ 0.60%), and their abundance on biofilms at high and low ammonium concentrations was 8.42% and 11.17%, respectively.
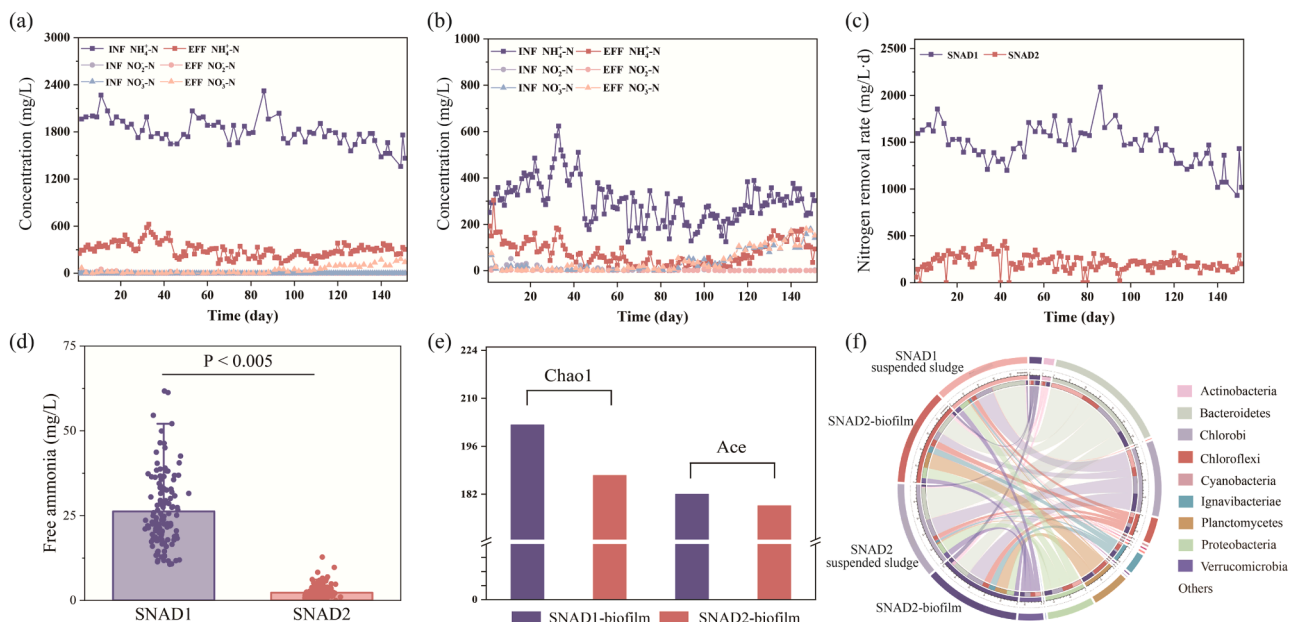

Fig. 1. The nitrogen concentration during the operation for (a) SNAD1 and (b) SNAD2 reactors. (c) Nitrogen removal rate (NRR) during the reactor operation for SNAD1 and SNAD2 reactors. (d) Statistical analysis of free ammonium (FA) concentration differences during the operation for SNAD1 and SNAD2 reactors. (e)The Ace and Chao1 indices of microbial communities on the biofilms of SNAD1 and SNAD2 reactors. (f) The relative abundance of recovered MAGs at the phylum level in SNAD1 and SNAD2 reactors.

Thus, the anammox consortia on the biofilms was further analyzed in this study. In total, 345 099 396 reads were generated from metagenomic sequencing, and then 340 542 882 reads were obtained after read quality control (Table S2). A total of 77 high-quality metagenome assembled genomes (MAGs) (completeness > 90%; contamination < 10%) were obtained. The ACE and Chao1 indices were applied to compare the species richness in different samples. As shown in Fig. 1e, the Ace (182.01) and Chao1 (202.3) indices on the SNAD1 reactor biofilm were higher than those (178.63 and 187.5) in the SNAD2 reactor, which corresponds to changes in nitrogen removal performance. The relative abundance of the anammox-related phylum *Planctomycetota* was higher in the SNAD1 reactor (15.41%) compared to the SNAD2 reactor (19.80%). At the genus level, the main detected genera of anammox bacteria were *Ca.Brocadia* and *Ca.Kuenenia*. A total of four MAGs (AMX1, AMX2, AMX3, AMX4) were identified as anammox bacteria, which were most similar to *Candidatus Brocadia* sp. *UTAMX1*, *Candidatus Brocadia fulgida*, *Candidatus Kuenenia stuttgartiensis* and *Candidatus Brocadia pituitae* (Table. S3). The average nucleotide identity (ANI) between the anammox MAGs we obtained and the reference genomes exceeded 95%.

At the phylum level, the dominant phyla detected in two reactors mainly included *Chlorobi, Bacteroidetes, Planctomycetota, Proteobacteria,*
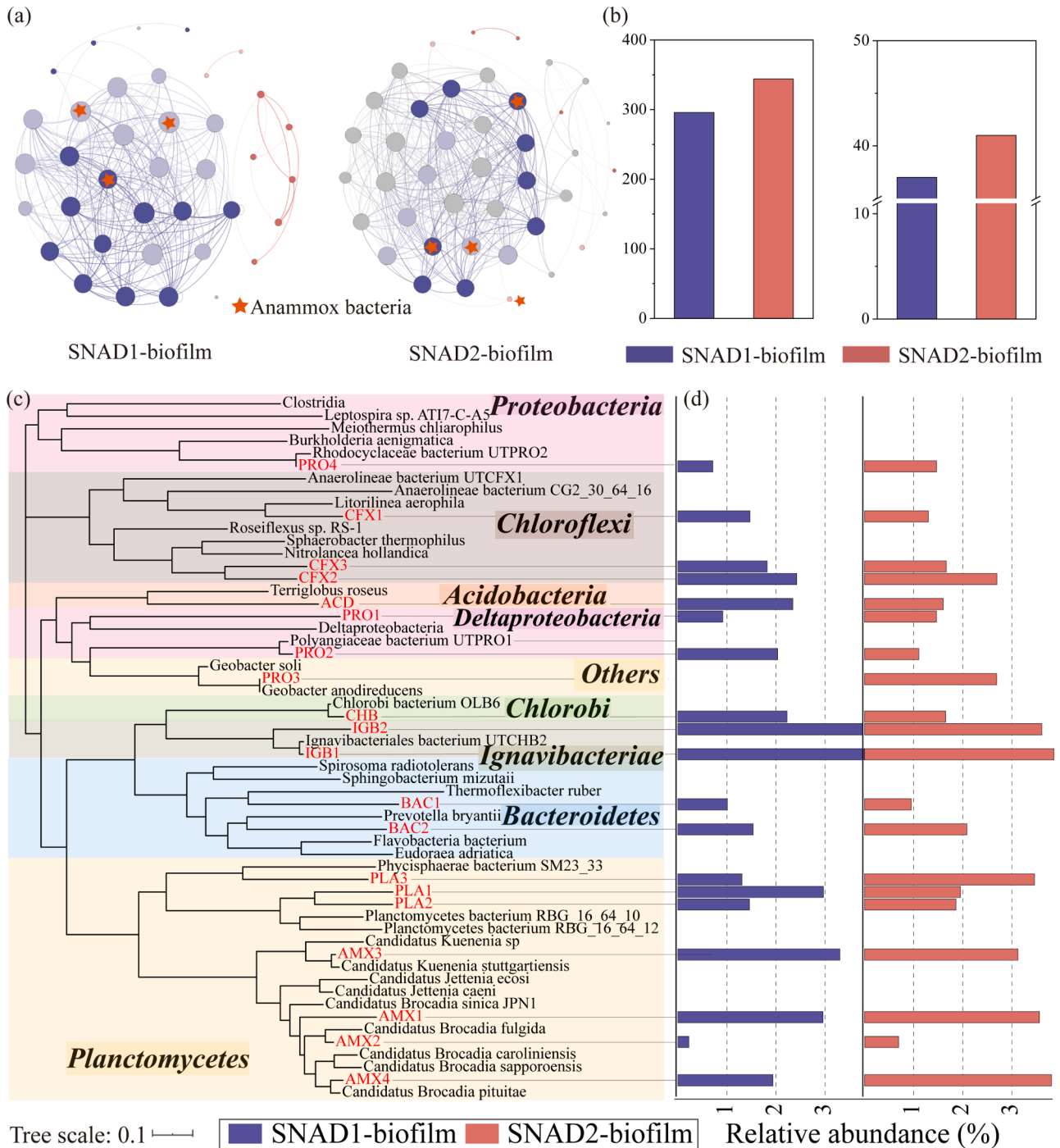

Fig. 2. (a) Co-occurrence network of bacteria with relative abundance greater than 1% in SNAD1 and SNAD2 reactors. (b) The number of nodes and edges of the co-occurrence network of SNAD1 and SNAD2 reactors. (c) Phylogenetic tree of the recovered draft genomes (red) and reference genomes (black) deposited in GenBank. (d) The relative abundance of anammox bacteria and symbiotic bacteria in SNAD1 and SNAD2 reactors.

Actinobacteria, Ignavibacteriae and *Chloroflexi* (Fig. 1f). *Chlorobi*-affiliated bacteria were the most abundant bacteria on the SNAD1 biofilm (22.44%), which was notably lower in the SNAD2 reactor (11.36%). The dominant bacteria belonged to the phyla *Bacteroidetes, Planctomycetes*, and *Proteobacteria*, with a slightly higher relative abundance in the SNAD2 reactor compared to that in the SNAD1 reactor.

2.2. Discrepant symbiotic bacteria of anammox bacteria under different ammonium concentrations

To investigate the effects of NH_4^+-N concentration on the microbial interactions in anammox consortia, two co-occurrence networks of biofilms in SNAD1 (NetB1) and SNAD2 (NetB2) reactor were constructed (Fig. 2a). Anammox bacteria in the WWTP were associated with a great diversity of symbiotic bacteria. In NetB1, there were 37 nodes connected by 296 links, whereas NetB2 exhibited 41 nodes with 344 links (Fig. 2b). The average degree of NetB2 (18.78) was higher than that of NetB1(15.32) (Fig. S1). The co-occurrence network was more complex and closely connected in biofilms of SNAD2 reactor compared to SNAD1 reactor (Fig.S1). We then focused on symbiotic bacteria that were connected to anammox bacteria in the co-occurrence network (Li et al., 2021) with a relative abundance greater than 1%. These symbiotic bacteria affiliated to phyla of *Proteobacteria, Chloroflexi, Acidobacteria, Deltaproteobacteria, Thermodesulfobacteriota, Chlorobi, Ignavibacteriae, Bacteroidetes*, and *Planctomycetes* (Fig. 2c, Table S3). PRO2, PRO4, CHB, and IGB1 were similar to *Polyangiaceae bacterium UTPRO1, Rhodocyclaceae bacterium UTPRO2, Chlorobi bacterium OLB6* and *Ignavibacteriales bacterium UTCHB2* (ANI > 95%) (Table S4). Notably, PRO4 belonged to the genus *Geobacter* and was a functional microorganism in the

Feammox process. The symbiotic bacteria associated with anammox bacteria in WWTP exhibited a wide range of species, distributed in nine phyla.

Using the functional gene abundance of COG class, the PCA analyzes demonstrated that the community structure within the anammox consortia was more complex in the SNAD1 reactor (Fig. 3). The MAGs that had similar gene abundances at the COG class level would colonize into a cluster. Notably, there were significant differences in the colonization-specific clusters and MAG composition between the two reactors. In detail, the SNAD1 reactor exhibited a higher number of clusters compared to the SNAD2 reactor (Fig. 3b–c). In SNAD1 reactor, CHB, PRO1, PRO2 and ACD were in one group (Group III) that separated from anammox bacteria. Two clusters were formed in the SNAD2 reactor, containing AMX2 (Group I) and AMX4 (Group IV), respectively. Anammox bacteria and symbiotic bacteria had distinct functional differences at the COG class level (Fig. 3d), as described in detail in the supplementary material.

The species composition of dominant symbiotic bacteria was distinct in two reactors. The relative abundances of ACD, CHB, PLA1, and PRO2 in SNAD1 biofilm were higher than those in SNAD2 reactor. These four MAGs were similar to *Terriglobus roseus, Chlorobi bacterium OLB6* (ANI > 99%), *Planctomycetes bacterium RBG_16_64_10* and *Polyangiaceae bacterium UTPRO1* (Fig. 2d, Table.S4). Conversely, the relative abundances of BAC2, PLA3, PRO1, PRO3, and PRO4 in the biofilm of the SNAD2 reactor were higher than those in the biofilm of the SNAD1 reactor. They belonged to the phylum *Bacteroidetes, Planctomycetes, Proteobacteria* and *Chloroflexi*. We specifically compared the dominant symbiotic bacteria with a significant difference in relative abundance between the two reactors (differences exceeding 30%) (Fig. S2). Specifically, ACD, CHB,
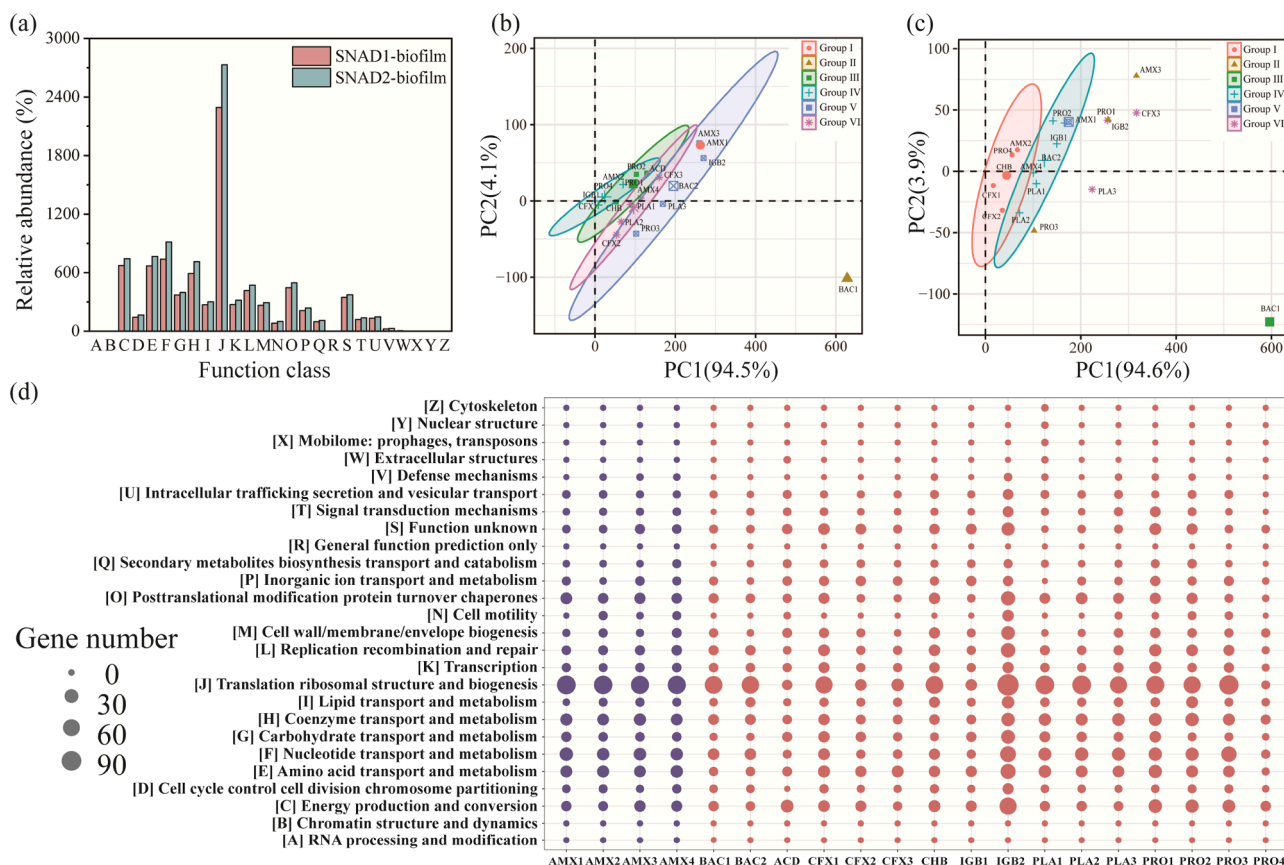

Fig. 3. (a) The total functional gene abundance on the level of COG classes in the recovered MAGs of anammox bacteria and symbiotic bacteria for two reactors. The community functional structure analysis using the PCA analysis of functional gene abundance on the COG classes level based on the sum of gene abundance of a certain COG class in every MAG in (b) SNAD1, (c) SNAD2, respectively. (d) Comparative analysis of gene numbers on the COG class level among recovered draft genomes of anammox bacteria and symbiotic bacteria.

PLA1, and PRO2 were dominant under high ammonium conditions in the SNAD1 reactor, while BAC2, PLA3, PRO1, PRO3, and PRO4 were dominant in the SNAD2 reactor.

The dominant symbiotic bacteria in SNAD1 reactor with high ammonium concentration could synthesize more types of amino acids compared to dominant symbiotic bacteria in SNAD2 reactor. It hinted that symbiotic bacteria require fewer types of amino acids provided by anammox bacteria under high ammonium condition. The dominant symbiotic bacteria in SNAD1 reactor had a complete pathway for synthesizing multiple amino acids (serine, alanine, glutamate, and proline) (Fig. 4a). In contrast, most of the dominant symbiotic bacteria in SNAD2 reactor lacked the capacity for amino acid synthesis. Most of dominant symbiotic bacteria (4/5) in SNAD2 reactor had insufficient capacity in the biosynthesis of serine, alanine, and proline. BAC2, PLA3, and PRO3 lacked the complete pathway for synthesizing glutamate. We downloaded reference genomes of these symbiotic bacteria and found they have the same deficiencies. Interestingly, anammox MAGs had a complete pathway to synthesize above amino acids. Furthermore, anammox MAGs and the majority of dominant symbiotic bacteria in SNAD1 reactor lacked a complete pathway for synthesizing tyrosine, while dominant symbiotic bacteria in SNAD2 reactor were capable of its synthesis. Anammox bacteria were unable to synthesize methionine and vitamin B6, but the dominant symbiotic bacteria of both two reactors had this function (Fig. S3). Moreover, the dominant symbiotic bacteria under high ammonium condition encoded more peptidases on the outer membrane for protein hydrolysis (Fig. 4b, Fig. S4). We revealed metabolic complementarity between anammox bacteria and symbiotic bacteria in terms of methionine, vitamin B6, and amino acids, suggesting

complex cross-feeding patterns among anammox consortia in the WWTP.

2.3. Increased growth rate of anammox bacteria after dosing vitamin B6

The addition of vitamin B6 enhanced the nitrogen removal performance and growth rate of anammox bacteria, as demonstrated by batch assays and model simulation. In the experimental groups with exogenous vitamin B6 addition and DO of 1 mg/L, the NRR of anammox consortia significantly increased by 43.5% ($P < 0.05$) (Fig. 5a). The degradation of NH_4^+-N and NO_2^--N was significantly accelerated with the addition of vitamin B6 (Fig. S5). The COBRA Toolbox for MATLAB with FBA were used to calculate the metabolic fluxes of anammox bacteria using the recovered genome from the WWTP (Table S3). The variation in metabolic fluxes of nucleotide metabolism reactions related to the reproduction rate of anammox bacteria was compared after adding vitamin B6 to the medium of anammox models. The number of reactions with increased metabolic fluxes (34) was greater than those with decreased metabolic fluxes (4) for nucleotide metabolism reactions (Fig. 5b). The growth rate of anammox bacteria increased from 40.61 to 77.39 mmol·g^{-1}·h^{-1} after the addition of vitamin B6 with an increase of 90.57% (Fig. 5c). The average flux of flux-increasing nucleotide metabolism pathways significantly increased by 1.69-fold for purine-related reactions and by 49.42-fold for pyrimidine-related reactions ($P < 0.05$) (Fig. 5d). For the adenosine triphosphate (ATP)-utilization reactions, the numbers of flux-increasing and flux-decreasing reactions were 39 and 13 after adding vitamin B6 to the medium (Fig. S6). The average flux of flux-increasing reactions increased by 3.31-fold with the presence of the
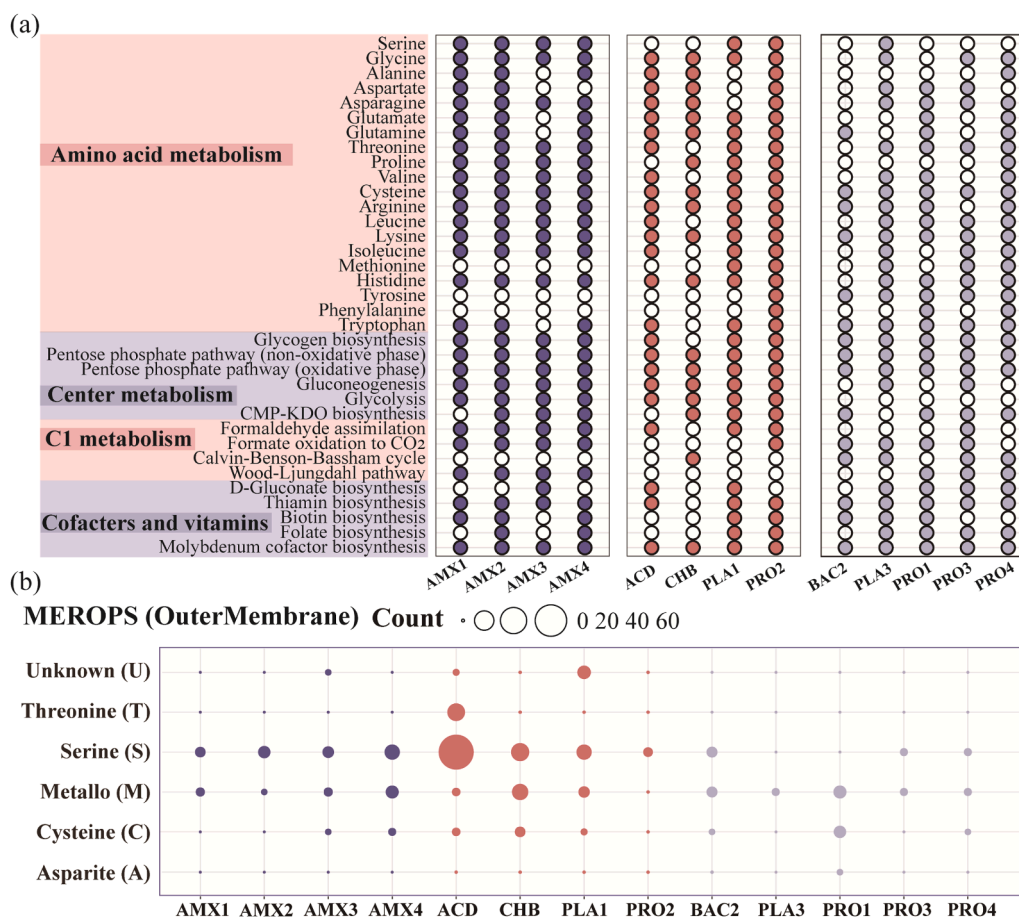

Fig. 4. (a) Pathway reconstructed from KEGG for recovered draft genomes of anammox bacteria and dominant symbiotic bacteria. Hollow dots represent the absence of this metabolic pathway. (b) Number (bubble diameter) of selected peptidase genes potentially involved in EPS matrix protein degradation in each genome of anammox bacteria and dominant symbiotic bacteria in two reactors.
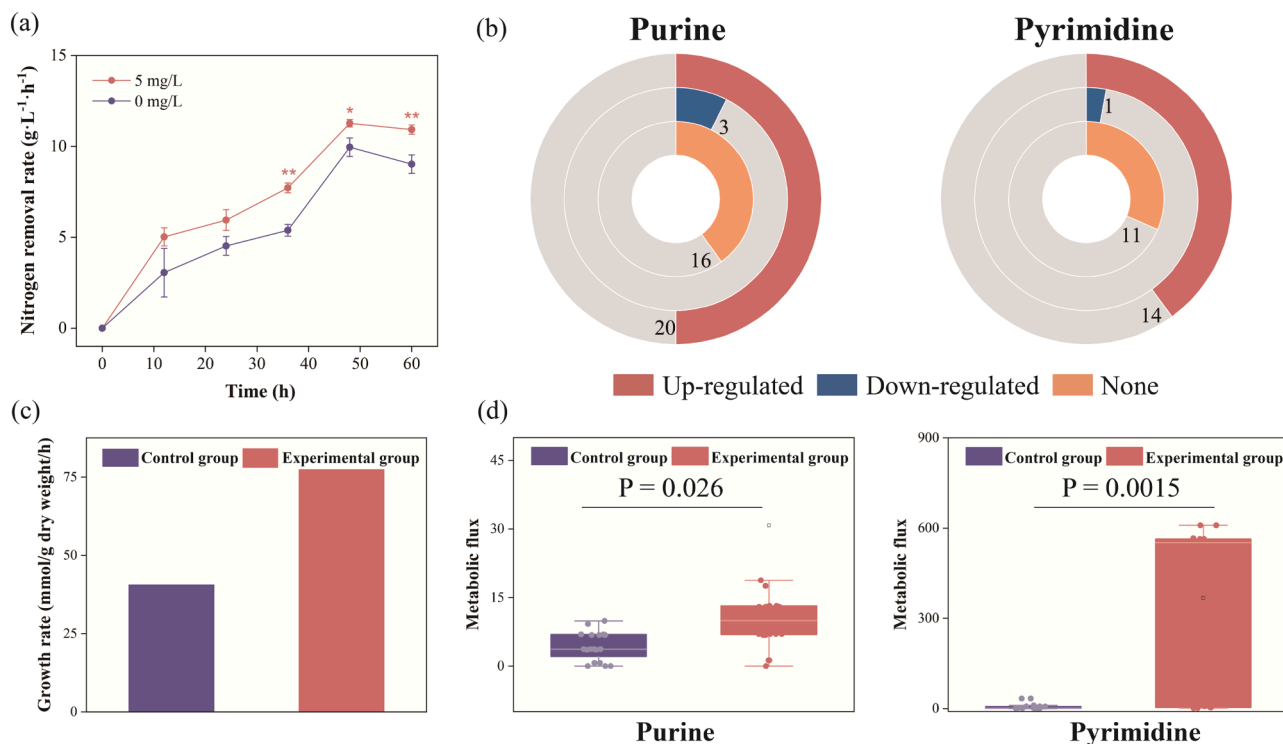
Fig. 5. (a) The nitrogen removal rate of anammox consortia after adding vitamin B6 to the medium. (b) The numbers of metabolic reactions that the metabolic flux changed of reactions in purine and pyrimidine pathways, (c) The growth rate of anammox bacteria calculated using the COBRA and FBA and (d) the statistical analysis of difference for the metabolic flux of reactions in purine and pyrimidine pathways after adding vitamin B6 in the medium during constructing the model.

vitamin B6. So, the metabolic energy consumption increased for higher activity after dosing vitamin B6 (Fig. S6).

2.4. Generalists shifted to specialists to resist to high ammonium

By identifying the topological roles of bacteria, we found that there were more specialists than generalists under high ammonium condition. The topological roles of nodes were defined by the within-module connectivity (Zi) and among-module connectivity (Pi). The MAGs in this study could be divided into two types. The first type was peripherals (specialists) with Zi and Pi values < 2.5 and 0.62, respectively. The remaining nodes were classified as connectors (generalists), which were nodes with Zi values < 2.5 and Pi values > 0.62 (Fig. 6a) (Mohamed et al., 2022). A total of 67.6% nodes were specialists and 32.4% nodes were generalists in NetB1. In contrast, in NetB2, generalists accounted for the majority (58.5%) and the number of specialists decreased (41.5%) (Fig. S7). In the SNAD1 reactor, the majority of specialists belong to the phyla *Planctomycetes, Proteobacteria, Acidobacteria* and *Chloroflexi*. There was a larger number of generalists in the SNAD2 reactor, mainly composed of bacteria belonging to the phyla *Planctomycetes* and *Ignavibacteria*. Notably, *Planctomycetes*-affiliated bacteria were more abundant as specialists in SNAD1 reactor (10.61%) compared to SNAD2 reactor (1.53%) (Fig.S6). Bacteria affiliated with the *Chlorobi* phylum were generalists in SNAD1 (20.22%), and shifted to specialists in the SNAD2 reactor (11.35%) (Fig. S8). AMX1, AMX3, AMX4 were identified as generalists in the NetB2 network but as specialists in the NetB1 network. Eight symbiotic bacteria were generalists in SNAD2 reactor and transitioned to specialists in SNAD1 reactor. Two out of four dominant symbiotic bacteria (CHB and PRO2) in SNAD1 reactor transitioned from generalists to specialists as ammonium condition in the reactor increased from 76.03 mg/L to 297.95 mg/L, while the topological roles of the rest two did not change. The transition to specialists occurred with an increase in abundance, suggesting that becoming specialists enhanced their competitive advantage. Then, we calculated

the node-level topological features. The degree, weighted degree, and eigencentrality of specialists were significantly higher ($P < 0.05$) than those of the generalists (Fig. 6b). There were more specialists than generalists under high ammonium condition with significant differences observed in the topological features between the two groups.

2.5. Great adaptation of Ca. Kuenenia to high ammonium condition

Ca.Kuenenia and *Ca.Brocadia* exhibit different abundance in two reactors. At the genus level, the main detected functional genera were *Ca. Brocadia* and *Ca.Kuenenia*. In both two reactors, the abundance of *Ca. Brocadia* was found to be higher than that of *Ca.Kuenenia*. As the NH_4^+-N concentration increased, the abundance of *Ca.Brocadia* decreased from 8.04% to 5.11% (Fig. 7). There was no significant difference in the abundance of *Ca.Kuenenia* in different reactors, which was 3.30% and 3.12% in the SNAD1 and SNAD2 reactors, respectively (Fig. 7). This illustrated that *Ca.Kuenenia* was more adaptable to changing NH_4^+-N concentrations than *Ca.Brocadia*. We compared the metabolic characteristics of *Ca.Kuenenia* and *Ca. Brocadia* through the KEGG database. The results showed that both genera of anammox bacteria possessed F-type ATPase and *Ca.Kuenenia* additionally possessed V/A-type ATPase, which *Ca.Brocadia* did not have. It suggested that *Ca.Kuenenia* is more adaptable to changes in ammonium concentration, since the V/A-type ATPase serve as the principal proton pumps accountable for acidification and pH regulation within intracellular compartments to resist cell alkalization caused by FA entering the cytoplasm (Fig. 6) (Ferreira et al., 2007; Forgac, 2007; Vasanthakumar and Rubinstein, 2020). While F-type ATPases primarily function in ATP synthesis in mitochondria and chloroplasts, and do not play a direct role in pH regulation (Kühlbrandt, 2019). Moreover, Cbb3-type cytochrome c oxidase (cbb3-type CcO) genes related to aerobic respiration capability of anammox bacteria were only present in *Ca.Kuenenia*. Additionally, *Ca.Kuenenia* exhibited higher values of degree and closnesscentrality in the co-occurrence network in SNAD1 reactor (Fig. S9). It indicated that *Ca.Kuenenia*
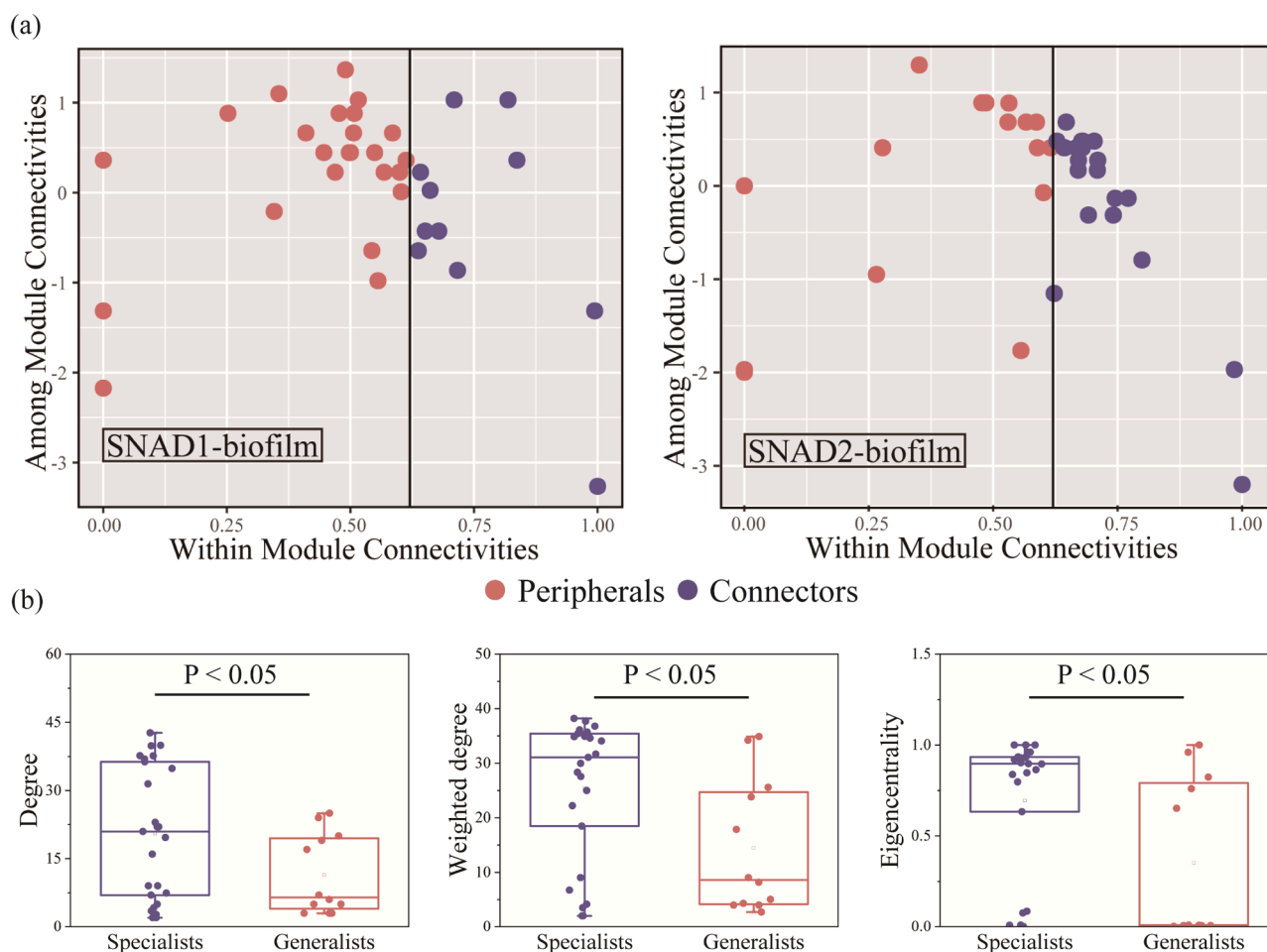
(a)

(b)

Fig. 6. (a) Zi-Pi plot showing the distribution of recovered MAGs according to their topological roles in SNAD1 and SNAD2 reactors. (b) Node-level topological features of the bacteria generalists and specialists in SNAD1 and SNAD2 reactors.

cooperated more with other bacteria to resist high ammonium conditions. V/A-type ATPase for anammox bacteria to adapt to the change of NH_4^+-N concentration was highly important to strive against cellular alkalization caused by free ammonia.

3. Discussion

3.1. Metabolic cross-feedings among anammox consortia in WWTPs

Anammox bacteria rely on the symbiotic bacteria to supply methionine and vitamin B6. Herein, we found the assembled anammox genomes all missing the complete pathway for methionine and vitamin B6 biosynthesis. Meanwhile, the assembled genomes deposited in the NCBI GenBank all lacked the complete pathway for methionine and vitamin B6 biosynthesis, including *Candidatus Brocadia fulgida* (JABAQY000000000), *Candidatus Brocadia pituitae* (AP021856), and *Candidatus Kuenenia stuttgartiensis* (SOES00000000). Vitamin B6 participates in hundreds of biochemical reactions in the cell as a coenzyme (Mooney et al., 2009), including amino acid synthesis (Adams et al., 2006) and fatty acid biosynthesis (Choudhury et al., 2010). Vitamin B6 also serves as a highly effective antioxidant, facilitating the removal of reactive oxygen species (Bilski et al., 2000; Parra et al., 2018). Methionine also contributes to enhancing bacterial oxidative tolerance (Gu et al., 2015). The results of batch assays showed that vitamin B6 promotes the nitrogen removal performance of anammox bacteria under the DO of 1 mg/L. We investigated the effect of vitamin B6 on the antioxidant capacity of anammox bacteria by adjusting DO levels and

found that vitamin B6 is beneficial for anammox bacteria in resisting oxygen-rich environments. The engineering significance of vitamin B6 in full-scale anammox reactors deserves further exploration in the future. According to the simulation of metabolic models, vitamin B6 also enhanced the growth rate of anammox bacteria as well as energy utilization. The increase in metabolic fluxes of ATP-utilization reactions indicated that vitamin B6 promotes the metabolic activity of anammox bacteria. Methionine is an essential amino acid that improves cellular oxidative balance and mediates oxidative stress (Gu et al., 2015). Symbiotic bacteria supply anammox bacteria with vitamin B6 and methionine, thereby reducing the metabolic costs of anammox bacteria. Although most studies of cross-feeding in anammox lab-scale reactors have been conducted in via of amino acids, glycogen, folate, etc. (Feng et al., 2019; Lawson et al., 2017; Zhao et al., 2018). Heterotrophic bacteria can degrade extracellular proteins produced by anammox bacteria to amino acids to affect consortium aggregation (Lawson et al., 2017; Zhao et al., 2018). Symbiotic bacteria provide folate to anammox bacteria, which promotes the growth rate of anammox bacteria and reduces their metabolic burden in anaerobic conditions (Zhao et al., 2018). Here, we revealed new cross-feedings of methionine and vitamin B6 that symbiotic bacteria provide to anammox bacteria, which helps anammox bacteria to adapt to the oxygen-containing environment of WWTPs.

We found Feammox bacteria are connected to anammox bacteria in the co-occurrence network in the WWTP. The symbiotic bacteria belong to *Chloroflexi, Chlorobi, Planctomycetes*, etc., are commonly found in anammox consortia (Zhao et al., 2018). In previous studies, PRO2
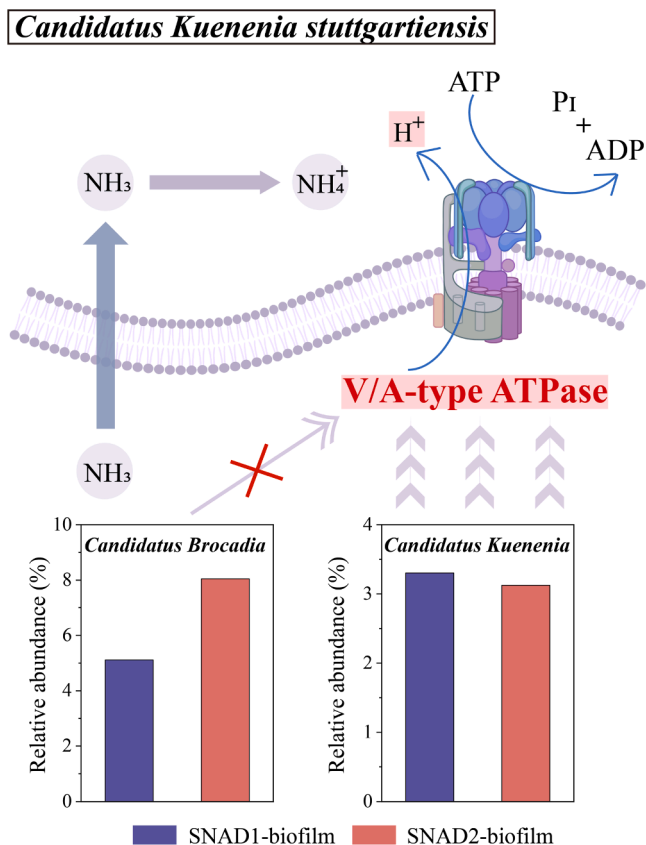
Fig. 7. Diagram explaining the mechanism of *Ca.Kuenenia* being better able to adapt to changes in NH_4^+-N concentration than *Ca.Brocadia*.

(*Polyangiaceae bacterium UTPRO1*), PRO4 (*Rhodocyclaceae bacterium UTPRO2*), CHB (*Chlorobi bacterium OLB6*), and IGB1 (*Ignavibacteriales bacterium UTCHB2*) were considered to facilitate a nitrite loop of anammox bacteria (Lawson et al., 2017). They participate in cross-feedings of amino acids and vitamins with anammox bacteria (Lawson et al., 2017). Here, we discovered that PRO3, belonging to the phylum *Thermodesulfobacteriota*, was classified as *Geobacter* at the genus level. *Geobacter* is an iron-reducing bacterium (Shaw et al., 2020) and play an important role in the Feammox process (Zhu et al., 2022), which refers to Fe (III) reduction coupled with anammox process (Butler et al., 2010; Yang et al., 2021). Fe (III) served as the electron acceptor in the reactor under anaerobic conditions. The NO^{2-}-N produced in the Feammox process can be utilized by the anammox bacteria to achieve effective nitrogen removal (Li et al., 2018; Piccardi et al., 2019). In this way, the cooperation of anammox and Feammox bacteria may contribute a lot to the autotrophic nitrogen removal in the WWTPs.

3.2. Microorganisms adapt to high ammonium by adjusting cross-feeding

Anammox bacteria tended to reduce the amino acids supply to symbiotic bacteria to save metabolic costs at high NH_4^+-N conditions. It has been reported that bacteria resist high ammonium strength by adjusting their metabolic mechanisms. Bacteria up-regulated the genes related to bacterial secretion and lipopolysaccharide synthesis to resist ammonia nitrogen stress (Weng et al., 2022). Heterotrophic nitrification-aerobic denitrification bacteria enhanced the carbon and nitrogen metabolism to cope with high levels of NH_4^+-N concentration (Guo et al., 2024). ACD, CHB, PLA1, and PRO2, which had fewer amino acid deficiencies than the dominant symbiotic bacteria in the SNAD2 reactor, predominated in the biofilm of the SNAD1 reactor. Anammox bacteria select symbiotic bacteria with fewer amino acid deficiencies, thereby saving metabolic energy to supply them amino acids for

adapting to high NH_4^+-N conditions. High level of NH_4^+-N inhibits the bacterial activity. Coral bacteria could respond to high NH_4^+-N stress by altering their co-occurrence patterns with bacterial members (Zhang et al., 2021b). The symbiotic bacteria may play an important role in resisting this high NH_4^+-N environment for anammox bacteria. Here we found anammox bacteria adapt to this adverse environment by changing their cross-feeding pattern with symbiotic bacteria. The dominant symbiotic bacteria with high relative abundance under low NH_4^+-N condition have more amino acid deficiencies (serine, alanine, glutamate, and proline), while the dominant symbiotic bacteria under high NH_4^+-N condition can synthesize these amino acids. The process of amino acid synthesis consumes metabolic energy (Kaleta et al., 2013).

Amino acids are essential for the growth and reproduction of microorganisms. The cross-feeding of amino acids between anammox bacteria and symbiotic bacteria enhances the activity of bacteria (Li et al., 2019). Here, we found anammox bacteria provide costly amino acids to symbiotic bacteria in exchange for methionine and vitamin B6 as resource feedback in this study. It was found that FA rather than ammonium itself, was the true inhibitor (Dapena-Mora et al., 2007). It was suggested that, in order to maintain the stable operation of the anammox system, the optimal concentration of FA was found to be less than 20–25 mg/L (Fernández et al., 2012; Jin et al., 2012). In this study, the concentration of FA in SNAD1 reactor reached 26.22 ± 5.45 mg/L, which is unfavorable for the survival of anammox bacteria. Under high ammonium condition, microorganisms also need to consume energy for antioxidant systems under FA stress (Chen et al., 2022b). After FA enters the cytoplasm, microorganisms consume energy using a potassium pump for proton balancing to maintain intracellular pH (Decrey et al., 2016; McQueen and Bailey, 1990). In this way, anammox bacteria reduce the metabolic cost of synthesizing amino acids for symbiotic bacteria under FA stress. Saving energy for essential metabolism is a strategy used by bacteria to resist adverse environments (Chen et al., 2022a; Li et al., 2022). As FA destroys the EPS of anammox consortia, the content of soluble substrates in the environment increases (Wang et al., 2018). Anammox bacteria can obtain methionine from the environment that they cannot synthesize themselves. This may also explain the higher abundance of *Chlorobi*-affiliated bacteria that catabolize extracellular peptides in the SNAD1 biofilms (Lawson et al., 2017). While *Candidatus Jettenia* actively exchanges costly amino acids as public goods under low nitrogen conditions (Guo et al., 2018), this behavior differs from that of *Ca.Brocadia* and *Ca.Kuenenia* observed in this study. This suggests that anammox bacteria of different genera use different strategies to cope with varying ammonium concentrations. Interestingly, the dominant bacteria in the SNAD1 reactor (CHB1 and ACD) had more threonine peptidases, serine peptidases and metallopeptidases. These peptidases have the function of transporting amino acids degraded from extracellular peptides into cells for their own growth and metabolism (Häse and Finkelstein, 1993; Siezen and Leunissen, 1997). Thus, they have the ability to obtain amino acids from the environment, resulting in a survival advantage under high NH_4^+-N condition.

3.3. Inspired specialists for community stability to resist to high ammonium

The transition from generalists to resource-efficient specialists could be a survival strategy for bacteria to resist adverse environments. Here, we found bacterial generalists transformed into specialists to resist to high ammonium. As reported, generalists and specialists exhibit significant discrepancy in resource utilization. Generalists are more versatile but less efficient than specialists, while specialists perform fewer activities more effectively (Chen et al., 2021). Generalists favor environments with high spatiotemporal heterogeneity, and specialists have an advantage in their optimal habitats (Kassen, 2002; Wilson and Yoshimura, 1994). Recent researches found specialists of fungi and bacteria exhibit more functions associated with nitrogen transformation and

organic matter degradation than generalist bacteria (Ren et al., 2023). Furthermore, generalists are detected to transition into specialists more frequently (Sriswasdi et al., 2017), such as the number of specialists is more abundant in high-hypersaline environments (Logares et al., 2013).

Correspondingly, the increased specialists ensure the stability and functional heterogeneity of the microbial community. The Ace and Chao1 indexes of microbial community were higher under high ammonium condition compared to the low ammonium condition in SNAD2 reactor, indicative of greater species richness and more diverse functionality. Community functional structure analysis showed that SNAD1 reactor has more clusters. Clave et al. proposed that the transition of more specialists to generalists promotes functional homogenization in biodiversity, potentially altering ecosystem functions and impacting biodiversity (Clavel et al., 2011). We further propose that the shift from generalists to specialists not only enhances functional heterogeneity but also contributes to ecosystem stability. Hence, these findings indicate that as the number of specialists increases under high ammonium condition, community functions become more diverse. Specialists have significantly higher degree, weighted degree, and eigencentrality than generalists (Fig. 2d, $P < 0.05$). Eigencentrality measures the influence of individual nodes on the network, while degree indicates the number of connections for each node (Dong et al., 2022). Higher values of these for specialists indicate that they are more frequently located centrally within the network and play a greater role in network stability than generalists (Yan et al., 2022). Therefore, it implies the potential role of specialists in maintaining microbial community stability. Improving the stability of the co-occurrence network helps the microbial community resist adverse environments (Ya et al., 2022). In this way, shift from generalists to specialists in SNAD1 reactor contributes to the stability of the bacterial co-occurrence network against high ammonium. Notably, a large number of anammox bacteria AMX1, AMX3, AMX4, and symbiotic bacteria shift from generalists to specialists in SNAD1 reactor, suggesting their important role in to maintaining ecosystem stability. The anammox process has significant advantages in energy saving and sludge reduction, while also reducing treatment costs and greenhouse gas emissions (Cruz et al., 2019; Wen et al., 2020). This study reveals the strategies of anammox bacteria to cope with high ammonium conditions and broadens our understanding of low-carbon and energy-saving anammox-based technology.

4. Conclusion

In this study, we found varied bacterial cooperation in anammox community to adapt to high ammonium in WWTP for treating sludge digestion liquid. Symbiotic bacteria provide methionine and vitamin B6 to anammox bacteria to enhance their antioxidant capacity in WWTP. Vitamin B6 promoted the growth rate and nitrogen removal performance of anammox bacteria. Anammox bacteria reduced the supply of amino acids to symbiotic bacteria under high NH_4^+-N condition to save their metabolic costs. Microorganisms transformed from generalists to specialists, thereby enhancing functional heterogeneity and stability of the microbial community to resist to high NH_4^+-N concentration. This study reveals bacterial survival strategies in response to high ammonium and provides new insights for understanding bacterial cooperations in WWTPs for low-carbon and energy-saving nitrogen removal.

5. Materials and methods

5.1. Reactor operation and sampling

The SNAD1 and SNAD2 reactor each had an effective volume of 832 m^3 to treat sludge digestion liquid located at China, Dalian. The reactor had an effective length, width and height of 16.0, 8.0 and 6.5 m, respectively, and was operated with a pH at 7.58 ± 0.9, DO of 0.5–1 mg/L and a temperature of 33.46 ± 3.69 °C. SNAD1 reactor and SNAD2 reactor are in series, and the effluent from SNAD1 reactor serves as the influent for SNAD2 reactor (Fig. S10). Influent and effluent samples were collected daily and analyzed immediately. Standard Methods for the Examinations of Water and Wastewater was used for measuring concentrations of NH_4^+-N, NO_2^--N, NO_3^--N (Rice et al., 2012). A pH meter (Sartorius PB-20, Germany) was used to determine the pH. Free ammonium (FA) concentration was calculated by equilibrium (Anthonisen et al., 1976). Samples were taken from the biofilms and suspended sludge of each reactor under stable operation with the nitrogen removal rate (NRR) of 1018.7 and 245.6 mg·L^{-1}·d^{-1}, respectively for the further analysis.

5.2. Batch assays

Batch assays were performed to measure the effect of vitamin B6 on the nitrogen removal performance of anammox bacteria. During the experiment, DO was maintained at 1 mg/L. The relative abundance of anammox bacteria in the inoculated anammox consortia was ~85% determined by fluorescence in situ hybridization (FISH) (Supplementary Methods, Fig. S11). The anammox medium (Supplementary Methods) used in batch assays contained 50 mg/L NO_2^--N, 50 mg/L NH_4^+-N for both control groups and experimental groups. Vitamin B6 of 5 mg/L was added to experimental groups. The concentration was determined based on previous study (Ryback et al., 2022) and model simulation results, which indicated that the exogenous addition of 5 mg/L of vitamin B6 had the most significant promotive effects on the growth of anammox bacteria. All treatments were performed in three replicates. The batch assays were performed with a constant temperature incubator stirring at 200 rpm while the culture temperature maintaining at 37 °C. Supernatant of 2 mL was collected every 12 h to determine the concentration of NH_4^+-N, NO_2^--N and NO_3^--N. The experiment lasted for 60 h until NH_4^+-N and NO_2^--N in the experimental groups or control groups were degraded completely.

5.3. Metagenome assembly, binning, and analysis

Detailed information on DNA extraction and metagenome sequencing is in Supplementary Methods. The raw Illumina reads could be found on the National Center for Biotechnology Information (NCBI) Web site under BioProject PRJNA1054297. Raw metagenomic reads were first trimmed with SeqPrep version 1.1, using default parameters to strip adapter sequences and ambiguous nucleotides (Robbins et al., 2011). Sickle version 1.33 was used as quality filter for the trimmed sequences with a minimum quality score of 20 and sequence length of 50 bp (Joshi and Sickle, 2011). IDBA-UD was used to assemble contigs and scaffolds individually for each sample based on default parameters (Peng et al., 2012). The generated scaffolds were binned into the draft genomes using MetaBAT version 0.32.5 based on the tetranucleotide frequency and abundance (Kang et al., 2015). The completeness and contamination of the draft genomes were measured by CheckM version 1.0.7 (Parks et al., 2015). The relative abundance of each draft genomes was calculated according to the method reported in the previous research (Lawson et al., 2017) using bbmap version 37.75 (https://sourceforge.net/projects/bbmap/).

OrthoANI version 0.93.1 (Lee et al., 2016) and BRIGersion0.95 (Lee et al., 2016) were used to calculate the average nucleotide identity of draft genomes and reference genomes.

5.4. Metabolic pathway reconstruction and metabolic potential analysis

Prodigal version 2.6.3 was used to annotate the open reading frames (ORFs) of each recovered draft genome based on a minimum nucleotide length of 60 (Hyatt et al., 2010). ORFs were annotated by eggNOG database and Kyoto Encyclopedia of Genes and Genomes pathway database (KEGG) with the blast e value of 1e−5. Through annotation by KEGG, metabolic pathways of draft genomes were reconstructed. Subsequently, metabolic complementarity between genomes was compared

based on metabolic pathways (Zhao et al., 2018). Peptidases were annotated against the MEROPS database (Rawlings et al., 2016). The subcellular localization predictor (CELLO version 2.5) (Yu et al., 2004) was used to predict the subcellular location (extracellular, outer membrane or periplasm) of each peptidase. This predictor employs support vector machines trained by multiple feature vectors derived from n-peptide composition to classify proteins (Yu et al., 2004). Principal component analysis (PCA) was used to establish the community functional structures in different reactors based on the abundance of functional genes within COG classes, as previously reported (Zhao et al., 2018). The PCA plot was displayed using the vegan package "factoextra" in R.

5.5. Phylogenetic identification of recovered draft genomes

Phylosift version 1.0.1 was used to construct the phylogenetic tree (Darling et al., 2014). The Phylosift "all" command was used to determine the taxa affiliations of recovered genomes. The marker genes of 28 reference genomes downloaded from National Center for Biotechnology Information (NCBI) were selected and used to build a phylogenetic tree (Table S1). The concatenated protein alignments of the reference genomes and the recovered genomes were aligned and re-concatenated using MAFFT version 7.310 (Daims et al., 2015; Katoh et al., 2002). Finally, a maximum likelihood phylogenetic tree was constructed using RAxML version 8.2.11 with 100 bootstraps (Stamatakis et al., 2008). The iTol tool was used to visualize the phylogenetic tree (Letunic and Bork, 2007).

5.6. Evaluation of the topological roles of bacteria

A co-occurrence network was constructed based on the Spearman correlation coefficient of bacterial abundance using "psych" package in R. Network visualization and topological characteristic calculation were conducted using the Gephi version 0.9.2 (Bastian et al., 2009). The "microeco" package in R was used to calculate within-module connectivity (Zi) and among-module connectivity (Pi) of each node. The threshold values of Zi and Pi for evaluating the topological roles of each node were 2.5 and 0.62, respectively (Bellafiore et al., 2005). We plotted scatter plots and bubble plots of the data using the "ggplot2" package in R. The alpha diversity (Ace and Chao1 indices) was calculated by the "vegan" package in R.

5.7. Flux balance analysis based on genome-scale metabolic models (GSMM)

GSMMs serve as mathematical representations of bacterial genotypes, depicting metabolic networks. They are utilized to generate mechanistic predictions regarding growth and resource allocation based on the bacterial culture media. It was used to predict cross-feedings between bacteria (Zhao et al., 2023). The GSMM of anammox bacteria was generated following the standard protocols (Pacheco et al., 2019). Firstly, the recovered genomes of anammox in this study was used to reconstruct metabolic models using Model SEED (http://modelseed.org/). The 'template model' option was set of 'gram negative' and the 'media' was set as the anammox medium. Then, the metabolic models were imported into MATLAB and the constraint-based reconstruction and analysis (COBRA) Toolbox was used for following steps. Finally, manual curation of models, prediction of growth rates, and estimation of metabolic fluxes of anammox models based on flux balance analysis (FBA) were performed.

CRediT authorship contribution statement

Yiming Feng: Writing – original draft, Visualization, Software, Investigation. **Lingrui Kong:** Software. **Ru Zheng:** Software. **Xiaogang Wu:** Investigation. **Jianhang Zhou:** Investigation. **Xiaochen Xu:**

Resources. **Sitong Liu:** Writing – review & editing, Investigation.

Declaration of competing interest

The authors declare that they have no known competing financial interests or personal relationships that could have appeared to influence the work reported in this paper.

Data availability

The raw metagenomics datasets have been deposited into National Center for Biotechnology Information (NCBI) Web site under BioProject PRJNA1054297.

Acknowledgements

Supplementary materials

Supplementary material associated with this article can be found, in the online version, at doi:10.1016/j.wroa.2024.100258.

References

Adams, J.B., George, F., Audhya, T., 2006. Abnormally high plasma levels of vitamin B6 in children with autism not taking supplements compared to controls not taking supplements. J. Altern. Complement. Med. 12 (1), 59–63.

Anthonisen, A., Loehr, R., Prakasam, T., Srinath, E., 1976. Inhibition of nitrification by ammonia and nitrous acid. J. Water. Pollut. Control Fed. 835–852.

Bastian, M., Heymann, S. and Jacomy, M. 2009 Gephi: an open source software for exploring and manipulating networks, pp. 361–362.

Bellafiore, S., Barneche, F., Peltier, G., Rochaix, J.-D., 2005. State transitions and light adaptation require chloroplast thylakoid protein kinase STN7. Nature 433 (7028), 892–895.

Bilski, P., Li, M., Ehrenshaft, M., Daub, M., Chignell, C., 2000. Vitamin B6 (pyridoxine) and its derivatives are efficient singlet oxygen quenchers and potential fungal antioxidants. Photochem. Photobiol. 71 (2), 129–134.

Butler, J.E., Young, N.D., Lovley, D.R., 2010. Evolution of electron transfer out of the cell: comparative genomics of six Geobacter genomes. BMC. Genomics. 11, 1–12.

Chen, C., Fang, Y., Cui, X., Zhou, D., 2022a. Effects of trace PFOA on microbial community and metabolisms: microbial selectivity, regulations and risks. Water. Res. 226, 119273.

Chen, Y.-J., Leung, P.M., Wood, J.L., Bay, S.K., Hugenholtz, P., Kessler, A.J., Shelley, G., Waite, D.W., Franks, A.E., Cook, P.L., 2021. Metabolic flexibility allows bacterial habitat generalists to become dominant in a frequently disturbed ecosystem. ISMe J. 15 (10), 2986–3004.

Chen, Z., Qiu, S., Li, M., Zhou, D., Ge, S., 2022b. Instant inhibition and subsequent self-adaptation of chlorella sp. Toward free ammonia shock in wastewater: physiological and genetic responses. Environ. Sci. Technol. 56 (13), 9641–9650.

Choudhury, S.R., Singh, S.K., Roy, S., Sengupta, D.N., 2010. An insight into the sequential, structural and phylogenetic properties of banana 1-aminocyclopropane-1-carboxylate synthase 1 and study of its interaction with pyridoxal-5'-phosphate and aminoethoxyvinylglycine. J. Biosci. 35, 281–294.

Clavel, J., Julliard, R., Devictor, V., 2011. Worldwide decline of specialist species: toward a global functional homogenization? Front. Ecol. Environ. 9 (4), 222–228.

Cruz, H., Law, Y.Y., Guest, J.S., Rabaey, K., Batstone, D., Laycock, B., Verstraete, W., Pikaar, I., 2019. Mainstream ammonium recovery to advance sustainable urban wastewater management. Environ. Sci. Technol. 53 (19), 11066–11079.

D'Souza, G., Shitut, S., Preussger, D., Yousif, G., Waschina, S., Kost, C., 2018. Ecology and evolution of metabolic cross-feeding interactions in bacteria. Nat. Prod. Rep. 35 (5), 455–488.

Daims, H., Lebedeva, E.V., Pjevac, P., Han, P., Herbold, C., Albertsen, M., Jehmlich, N., Palatinszky, M., Vierheilig, J., Bulaev, A., 2015. Complete nitrification by Nitrospira bacteria. Nature 528 (7583), 504–509.

Dapena-Mora, A., Fernandez, I., Campos, J., Mosquera-Corral, A., Mendez, R., Jetten, M., 2007. Evaluation of activity and inhibition effects on Anammox process by batch tests based on the nitrogen gas production. Enzyme Microb. Technol. 40 (4), 859–865.

Darling, A.E., Jospin, G., Lowe, E., Matsen, F.A., Bik, H.M., Eisen, J.A., 2014. PhyloSift: phylogenetic analysis of genomes and metagenomes. PeerJ. 2.

Decrey, L., Kazama, S., Kohn, T.J.A., 2016. Ammonia as an in situ sanitizer: influence of virus genome type on inactivation. Appl. Environ. Microbiol. 82 (16), 4909–4920.

Dong, K., Yu, Z., Kerfahi, D., Lee, S.-s., Li, N., Yang, T., Adams, J.M, 2022. Soil microbial co-occurrence networks become less connected with soil development in a high Arctic glacier foreland succession. Sci. Total. Environ. 813, 152565.

Feng, Y., Zhao, Y., Jiang, B., Zhao, H., Wang, Q., Liu, S., 2019. Discrepant gene functional potential and cross-feedings of anammox bacteria Ca. Jettenia caeni and Ca. Brocadia sinica in response to acetate. Water. Res. 165, 114974.

Fernández, I., Dosta, J., Fajardo, C., Campos, J., Mosquera-Corral, A., Méndez, R., 2012. Short-and long-term effects of ammonium and nitrite on the Anammox process. J. Environ. Manage. 95, S170–S174.

Ferreira, T., Carrondo, M., Alves, P., 2007. Effect of ammonia production on intracellular pH: consequent effect on adenovirus vector production. J. Biotechnol. 129 (3), 433–438.

Flemming, H.-C., Wingender, J., Szewzyk, U., Steinberg, P., Rice, S.A., Kjelleberg, S., 2016. Biofilms: an emergent form of bacterial life. Nat. Rev. Microbiol. 14 (9), 563–575.

Forgac, M., 2007. Vacuolar ATPases: rotary proton pumps in physiology and pathophysiology. Nat. Rev. Mol. Cell. Biol. 8 (11), 917–929.

Freilich, S., Zarecki, R., Eilam, O., Segal, E.S., Henry, C.S., Kupiec, M., Gophna, U., Sharan, R., Ruppin, E., 2011. Competitive and cooperative metabolic interactions in bacterial communities. Nat. Commun. 2 (1), 589.

Gad, M., et al., 2020. Distinct mechanisms underlying the assembly of microeukaryotic generalists and specialists in an anthropogenically impacted river. Sci. Total Environ. 748, 141434.

Gallert, C., Bauer, S., Winter, J.J.A.m., 1998. Effect of ammonia on the anaerobic degradation of protein by a mesophilic and thermophilic biowaste population. Appl. Microbiol. 50, 495–501.

Gu, S.X., Stevens, J.W., Lentz, S.R., 2015. Regulation of thrombosis and vascular function by protein methionine oxidation. Blood 125 (25), 3851–3859.

Guo, L., Li, L., Zhou, S., Xiao, P., Zhang, L., 2024. Metabolomic insight into regulatory mechanism of heterotrophic bacteria nitrification-aerobic denitrification bacteria to high-strength ammonium wastewater treatment. Bioresour. Technol. 394, 130278.

Guo, Y., Zhao, Y., Zhu, T., Li, J., Feng, Y., Zhao, H., Liu, S., 2018. A metabolomic view of how low nitrogen strength favors anammox biomass yield and nitrogen removal capability. Water. Res. 143, 387–398.

Häse, C., Finkelstein, R.A., 1993. Bacterial extracellular zinc-containing metalloproteases. Microbiol. Rev. 57 (4), 823–837.

Hu, P., Qian, Y., Liu, J., Gao, L., Li, Y., Xu, Y., Wu, J., Hong, Y., Ford, T., Radian, A., 2023. Delineation of the complex microbial nitrogen-transformation network in an anammox-driven full-scale wastewater treatment plant. Water. Res. 235, 119799.

Hyatt, D., Chen, G.-L., LoCascio, P.F., Land, M.L., Larimer, F.W., Hauser, L.J., 2010. Prodigal: prokaryotic gene recognition and translation initiation site identification. BMC Bioinf 11, 1–11.

Jin, R.-C., Yang, G.-F., Yu, J.-J., Zheng, P., 2012. The inhibition of the Anammox process: a review. Chem. Eng. J. 197, 67–79.

Joshi, N. and Sickle, F. 2011 A sliding-window, adaptive, quality-based trimming tool for FastQ files.

Kaleta, C., Schäuble, S., Rinas, U., Schuster, S., 2013. Metabolic costs of amino acid and protein production in Escherichia coli. Biotechnol. J. 8 (9), 1105–1114.

Kallistova, A., Nikolaev, Y., Grachev, V., Beletsky, A., Gruzdev, E., Kadnikov, V., Dorofeev, A., Berestovskaya, J., Pelevina, A., Zekker, I.J.F.i.M., 2022. New insight into the interspecies shift of anammox bacteria Ca."Brocadia" and Ca."Jettenia" in reactors fed with formate and folate. Front. Microbiol. 12, 802201.

Kang, D.D., Froula, J., Egan, R., Wang, Z., 2015. MetaBAT, an efficient tool for accurately reconstructing single genomes from complex microbial communities. PeerJ. 3, e1165.

Kartal, B., Kuenen, J.v., Van Loosdrecht, M., 2010. Sewage treatment with anammox. Science (1979) 328 (5979), 702–703.

Kassen, R., 2002. The experimental evolution of specialists, generalists, and the maintenance of diversity. J. Evol. Biol. 15 (2), 173–190.

Katoh, K., Misawa, K., Kuma, K.i., Miyata, T., 2002. MAFFT: a novel method for rapid multiple sequence alignment based on fast Fourier transform. Nucleic. Acids. Res. 30 (14), 3059–3066.

Kühlbrandt, W., 2019. Structure and mechanisms of F-type ATP synthases. Annu. Rev. Biochem. 88 (1), 515–549.

Lawson, C.E., Wu, S., Bhattacharjee, A.S., Hamilton, J.J., McMahon, K.D., Goel, R., Noguera, D.R., 2017. Metabolic network analysis reveals microbial community interactions in anammox granules. Nat. Commun. 8 (1), 15416.

Lee, I., Ouk Kim, Y., Park, S.-C., Chun, J., 2016. OrthoANI: an improved algorithm and software for calculating average nucleotide identity. Int. J. Syst. Evol. Microbiol. 66 (2), 1100–1103.

Letunic, I., Bork, P., 2007. Interactive Tree Of Life (iTOL): an online tool for phylogenetic tree display and annotation. Bioinformatics. 23 (1), 127–128.

Levins, R., 1968. Evolution in Changing Environments: Some Theoretical Explorations. Princeton University Press.

Li, J., Peng, Y., Zhang, L., Liu, J., Wang, X., Gao, R., Pang, L., Zhou, Y., 2019. Quantify the contribution of anammox for enhanced nitrogen removal through metagenomic analysis and mass balance in an anoxic moving bed biofilm reactor. Water. Res. 160, 178–187.

Li, W., Siddique, M.S., Graham, N., Yu, W., 2022. Influence of temperature on biofilm formation mechanisms using a gravity-driven membrane (GDM) system: insights from microbial community structures and metabolomics. Environ. Sci. Technol. 56 (12), 8908–8919.

Li, X., Huang, Y., Liu, H.-w., Wu, C., Bi, W., Yuan, Y., Liu, X., 2018. Simultaneous Fe (III) reduction and ammonia oxidation process in Anammox sludge. J. Environ. Sci. 64, 42–50.

Li, Y.-X., Rao, Y.-Z., Qi, Y.-L., Qu, Y.-N., Chen, Y.-T., Jiao, J.-Y., Shu, W.-S., Jiang, H., Hedlund, B.P., Hua, Z.-S., 2021. Deciphering symbiotic interactions of "Candidatus Aenigmarchaeota" with inferred horizontal gene transfers and co-occurrence networks. mSystems. 6 (4), 00606–00621. https://doi.org/10.1128/msystems.

Logares, R., Lindström, E.S., Langenheder, S., Logue, J.B., Paterson, H., Laybourn-Parry, J., Rengefors, K., Tranvik, L., Bertilsson, S., 2013. Biogeography of bacterial communities exposed to progressive long-term environmental change. ISMe J. 7 (5), 937–948.

McQueen, A., Bailey, J.E., 1990. Effect of ammonium ion and extracellular pH on hybridoma cell metabolism and antibody production. Biotechnol. Bioeng. 35 (11), 1067–1077.

Mohamed, T.A., Wu, J., Zhao, Y., Elgizawy, N., El Kholy, M., Yang, H., Zheng, G., Mu, D., Wei, Z., 2022. Insights into enzyme activity and phosphorus conversion during kitchen waste composting utilizing phosphorus-solubilizing bacterial inoculation. Bioresour. Technol. 362, 127823.

Mooney, S., Leuendorf, J.-E., Hendrickson, C., Hellmann, H., 2009. Vitamin B6: a long known compound of surprising complexity. Molecules. 14 (1), 329–351.

Ni, S.-Q., Zhang, J., 2013. Anaerobic ammonium oxidation: from laboratory to full-scale application. Biomed. Res. Int. 2013 (1), 469360.

Okada, U., Yamashita, E., Neuberger, A., Morimoto, M., van Veen, H.W., Murakami, S., 2017. Crystal structure of tripartite-type ABC transporter MacB from Acinetobacter baumannii. Nat. Commun. 8 (1), 1336.

Oña, L., Giri, S., Avermann, N., Kreienbaum, M., Thormann, K.M., Kost, C., 2021. Obligate cross-feeding expands the metabolic niche of bacteria. Nat. Ecol. Evol. 5 (9), 1224–1232.

Oña, L., Kost, C., 2022. Cooperation increases robustness to ecological disturbance in microbial cross-feeding networks. Ecol. Lett. 25 (6), 1410–1420.

Pacheco, A.R., Moel, M., Segrè, D., 2019. Costless metabolic secretions as drivers of interspecies interactions in microbial ecosystems. Nature Com 10 (1), 103.

Pande, S., Kaftan, F., Lang, S., Svatoš, A., Germerodt, S., Kost, C., 2016. Privatization of cooperative benefits stabilizes mutualistic cross-feeding interactions in spatially structured environments. ISMe J. 10 (6), 1413–1423.

Parks, D.H., Imelfort, M., Skennerton, C.T., Hugenholtz, P., Tyson, G.W., 2015. CheckM: assessing the quality of microbial genomes recovered from isolates, single cells, and metagenomes. Genome Res. 25 (7), 1043–1055.

Parra, M., Stahl, S., Hellmann, H., 2018. Vitamin B6 and its role in cell metabolism and physiology. Cells 7 (7), 84.

Peng, Y., Leung, H.C., Yiu, S.-M., Chin, F.Y., 2012. IDBA-UD: a de novo assembler for single-cell and metagenomic sequencing data with highly uneven depth. Bioinformatics. 28 (11), 1420–1428.

Piccardi, P., Vessman, B., Mitri, S., 2019. Toxicity drives facilitation between 4 bacterial species. Proc. Natl. Acad. Sci. U. S. A. 116 (32), 15979–15984.

Preussger, D., Giri, S., Muhsal, L.K., Oña, L., Kost, C., 2020. Reciprocal fitness feedbacks promote the evolution of mutualistic cooperation. Curr. Biol. 30 (18), 3580–3590 e3587.

Prosser, J.I., Bohannan, B.J., Curtis, T.P., Ellis, R.J., Firestone, M.K., Freckleton, R.P., Green, J.L., Green, L.E., Killham, K., Lennon, J.J., 2007. The role of ecological theory in microbial ecology. Nat. Rev. Microbiol. 5 (5), 384–392.

Rawlings, N.D., Barrett, A.J., Finn, R., 2016. Twenty years of the MEROPS database of proteolytic enzymes, their substrates and inhibitors. Nucleic. Acids. Res. 44 (D1), D343–D350.

Ren, D., Madsen, J.S., Sørensen, S.J., Burmølle, M., 2015. High prevalence of biofilm synergy among bacterial soil isolates in cocultures indicates bacterial interspecific cooperation. ISMe J. 9 (1), 81–89.

Ren, Y., Ge, W., Dong, C., Wang, H., Zhao, S., Li, C., Xu, J., Liang, Z., Han, Y., 2023. Specialist species of fungi and bacteria are more important than the intermediate and generalist species in near-urban agricultural soils. Appl. Soil Ecol. 188, 104894.

Rice, E.W., Bridgewater, L., Association, A.P.H., 2012. Standard Methods for the Examination of Water and Wastewater. American public health association, Washington, DC.

Robbins, S.J., Chan, C.X., Messer, L.F., Singleton, C.M., Geers, A.U., Ying, H., Baker, A., Bell, S.C., Morrow, K.M. and Ragan, M.A. 2011. jstjohn/SeqPrep: tool for stripping adaptors and/or merging paired reads with overlap into single reads.

Rocha-Granados, M.C., Zenick, B., Englander, H.E., Mok, W.W., 2020. The social network: impact of host and microbial interactions on bacterial antibiotic tolerance and persistence. Cell. Signall. 75, 109750.

Ryback, B., Bortfeld-Miller, M., Vorholt, J.A., 2022. Metabolic adaptation to vitamin auxotrophy by leaf-associated bacteria. ISMe J. 16 (12), 2712–2724.

Shaw, D.R., Ali, M., Katuri, K.P., Gralnick, J.A., Reimann, J., Mesman, R., van Niftrik, L., Jetten, M.S., Saikaly, P.E., 2020. Extracellular electron transfer-dependent anaerobic oxidation of ammonium by anammox bacteria. Nat. Commun. 11 (1), 2058.

Siezen, R.J., Leunissen, J.A., 1997. Subtilases: the superfamily of subtilisin-like serine proteases. Protein Sci. 6 (3), 501–523.

Sriswasdi, S., Yang, C.-c., Iwasaki, W., 2017. Generalist species drive microbial dispersion and evolution. Nat. Commun. 8 (1), 1162.

Stamatakis, A., Hoover, P., Rougemont, J., 2008. A rapid bootstrap algorithm for the RAxML web servers. Syst. Biol. 57 (5), 758–771.

Vasanthakumar, T., Rubinstein, J.L., 2020. Structure and Roles of V-type ATPases. Trends. Biochem. Sci. 45 (4), 295–307.

Wang, D., Duan, Y., Yang, Q., Liu, Y., Ni, B.-J., Wang, Q., Zeng, G., Li, X., Yuan, Z., 2018. Free ammonia enhances dark fermentative hydrogen production from waste activated sludge. Water. Res. 133, 272–281.

Wen, R., Jin, Y. and Zhang, W. 2020 Application of the Anammox in China—a review.

Weng, X., Mao, Z., Fu, H.-M., Chen, Y.-P., Guo, J.-S., Fang, F., Xu, X.-W., Yan, P., 2022. Biofilm formation during wastewater treatment: motility and physiological response

of aerobic denitrifying bacteria under ammonia stress based on surface plasmon resonance imaging. Bioresour. Technol. 361, 127712.

Wilson, D.S., Yoshimura, J., 1994. On the coexistence of specialists and generalists. Am. Nat. 144 (4), 692–707.

Wimp, G.M., Ries, L., Lewis, D., Murphy, S.M., 2019. Habitat edge responses of generalist predators are predicted by prey and structural resources. Ecology. 100 (6), e02662.

Xu, Q., Luo, G., Guo, J., Xiao, Y., Zhang, F., Guo, S., Ling, N., Shen, Q., 2022. Microbial generalist or specialist: intraspecific variation and dormancy potential matter. Mol. Ecol. 31 (1), 161–173.

Ya, T., Liu, J., Zhang, M., Wang, Y., Huang, Y., Hai, R., Zhang, T., Wang, X., 2022. Metagenomic insights into the symbiotic relationship in anammox consortia at reduced temperature. Water. Res. 225, 119184.

Yan, Q., Liu, Y., Hu, A., Wan, W., Zhang, Z., Liu, K., 2022. Distinct strategies of the habitat generalists and specialists in sediment of Tibetan lakes. Environ. Microbiol. 24 (9), 4153–4166.

Yang, Y., Xiao, C., Yu, Q., Zhao, Z., Zhang, Y., 2021. Using Fe (II)/Fe (III) as catalyst to drive a novel anammox process with no need of anammox bacteria. Water. Res. 189, 116626.

Yu, C.S., Lin, C.J., Hwang, J.K., 2004. Predicting subcellular localization of proteins for Gram-negative bacteria by support vector machines based on n-peptide compositions. Protein. Sci. 13 (5), 1402–1406.

Zhang, S., Mukherji, R., Chowdhury, S., Reimer, L., Stallforth, P., 2021a. Lipopeptide-mediated bacterial interaction enables cooperative predator defense. Proc. Natl. Acad. Sci. U.S.A. 118 (6), e2013759118.

Zhang, Y., Yang, Q., Zhang, Y., Ahmad, M., Ling, J., Tang, X., Dong, J., 2021b. Shifts in abundance and network complexity of coral bacteria in response to elevated ammonium stress. Sci. Total Environ. 768, 144631.

Zhao, Y., Feng, Y., Zhou, J., Zhang, K., Sun, J., Wang, L., Liu, S., 2023. Potential bacterial isolation by dosing metabolites in cross-feedings. Water. Res. 231, 119589.

Zhao, Y., Liu, S., Jiang, B., Feng, Y., Zhu, T., Tao, H., Tang, X., Liu, S., 2018. Genome-centered metagenomics analysis reveals the symbiotic organisms possessing ability to cross-feed with anammox bacteria in anammox consortia. Environ. Sci. Technol. 52 (19), 11285–11296.

Zhu, J., Yan, X., Zhou, L., Li, N., Liao, C., Wang, X., 2022. Insight of bacteria and archaea in Feammox community enriched from different soils. Environ. Res. 203, 111802.

Zhuang, J.-L., Sun, X., Zhao, W.-Q., Zhang, X., Zhou, J.-J., Ni, B.-J., Liu, Y.-D., Shapleigh, J.P., Li, W., 2022. The anammox coupled partial-denitrification process in an integrated granular sludge and fixed-biofilm reactor developed for mainstream wastewater treatment: performance and community structure. Water. Res. 210, 117964.